Penerbit Akademia Baru

Journal of Advanced Research in Applied Mechanics
ISSN (online): 2289-7895 | Vol. 10, No. 1. Pages 9-29, 2015

Finding the Drilling Induced Fractures and Borehole Breakout Directions Using Image Logs

M. Alizadeh[*,1,a], *Z. Movahed*[1,b], *R. Junin*[1,c], *R. Mohsin*[1,d], *M. Alizadeh*[2,e] *and M. Alizadeh*[3,f]

[1]Faculty of Petroleum and Renewable Energy Engineering, Universiti Teknologi Malaysia, 81310 Johor, Malaysia
[2]Gachsaran Oil and Gas Production Company – GOGPC, 75818738 49 Gachsaran, Iran
[3]Mechanical Engineering Department, Tarbiat Modares University, 14155-111 Tehran, Iran
[a,*]*mostafa.alizadeh88@yahoo.com*, [b]*zmovahed@gmail.com*, [c]*radzuan@petroleum.utm.my*, [d]*rahmat@petroleum.utm.my*, [e]*alizadeh.me@gmail.com*, [f]*ymohsen.alizadeh@yahoo.com*

Abstract – *By interpreting image logs, both the directions of drilling induced fractures parallel to the maximum horizontal in-situ stress direction and borehole breakouts parallel to the minimum horizontal in-situ stress direction can be calculated. In this work, 10 wells located in Gachsaran field were selected then the direction of drilling induced fractures and borehole breakouts in these wells was examined by using image logs and other geological log interpretation. This work was done in order to have a better understanding of structural geology in this field and also explain the methodology by showing the selected log interpretation examples from this field.*

Keywords: Image logs, drilling induced fractures, borehole breakouts

1.0 INTRODUCTION

Gachsaran oil field is in the southwest of Iran (Figure 1) with an anticline structure, made of anhydrite/salt, 80 km long, 300m-1500m thickness, 8-18 km wide. It provides an excellent seal for the Asmari, Pabdeh, Gurpi and other reservoirs (Figure 2) [1].

2.0 MATERIAL AND METHODS

The main data for this job are the image log data including the Formation Micro Scanner (FMS), Oil-Base-Mud Imaging (OBMI), Formation Micro Imager (FMI) and the Ultrasonic Borehole Imager (UBI). In this work, 10 wells (GS-A, GS-B, GS-C, GS-D, GS-E, GS-F, GS-G, GS-H, GS-I and GS-G), located in the Gachsaran oil field were studied.

Maximum horizontal in-situ stress (σ_{hmax}) direction is the same as the induced drilling fracture direction, and minimum horizontal in-situ stress (σ_{hmin}) direction is the same as the borehole breakout direction. Both drilling induced fractures and borehole breakouts are created during the drilling operation [8].

Drilling induced fracture and borehole breakouts are different in images. The drilling induced fracture is in the form of a fracture seen by the images, oriented at 180 degrees from each side of the well, but borehole breakout is in the form of borehole elongation on the orthogonal calipers and as long dark regions on the images that are 180 degrees apart (Figure 3).

Penerbit Akademia Baru

Journal of Advanced Research in Applied Mechanics
ISSN (online): 2289-7895 | Vol. 10, No. 1. Pages 9-29, 2015

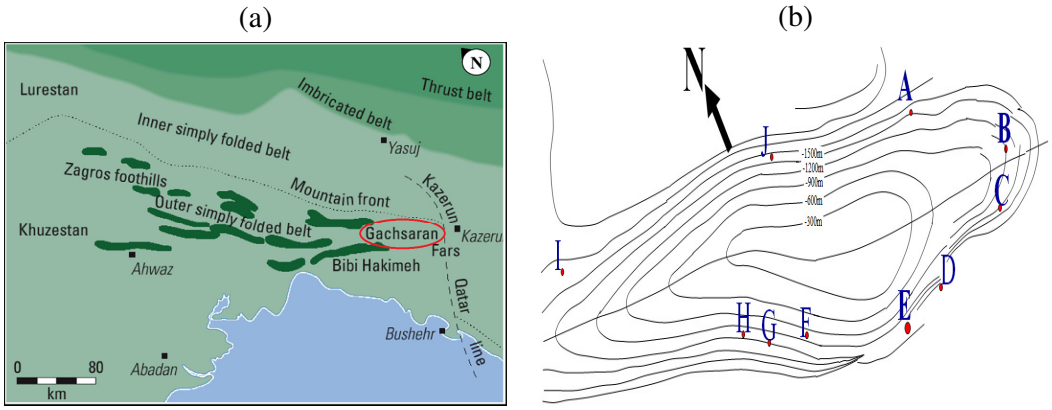

Figure 1: a) Location of the Gachsaran field [2]; b) UGC map of the Gachsaran field and the studied wells.

Image log technology is a new technology that can characterize oil and gas reservoirs in many cases such as structural analysis, fracture characterization, fault interpretation and in-situ stress analysis [3, 4]. These applications are still unknown to some researchers who are interested in learning the way that the in-situ stresses direction can be driven from image logs. Thus, this process will be explained completely in this job using a case study and numbers of valuable log interpretation [5-7].

3.0 THEORY

The borehole breakouts are due to the hoop stress that causes shear failure in the borehole, while the drilling induced fractures are due to the radial stress that causes the tensile failure in borehole. By uncovering the direction of induced drilling fractures and borehole breakouts from the image logs, we can locate the direction of in-situ stresses.

In wellbore there are always hoop stress and radial stress which cause drilling induced fracture and borehole breakouts. However, it depends on the rock strength in any part of the wellbore for any breakout to happen. If the rock strength is low the drilling fluid will wash the rock and borehole breakout will occur, but if the rock strength is high the drilling fluid will cause drilling induced fractures (hydraulic fractures) (Figure 4).

Penerbit Akademia Baru

Journal of Advanced Research in Applied Mechanics
ISSN (online): 2289-7895 | Vol. 10, No. 1. Pages 9-29, 2015

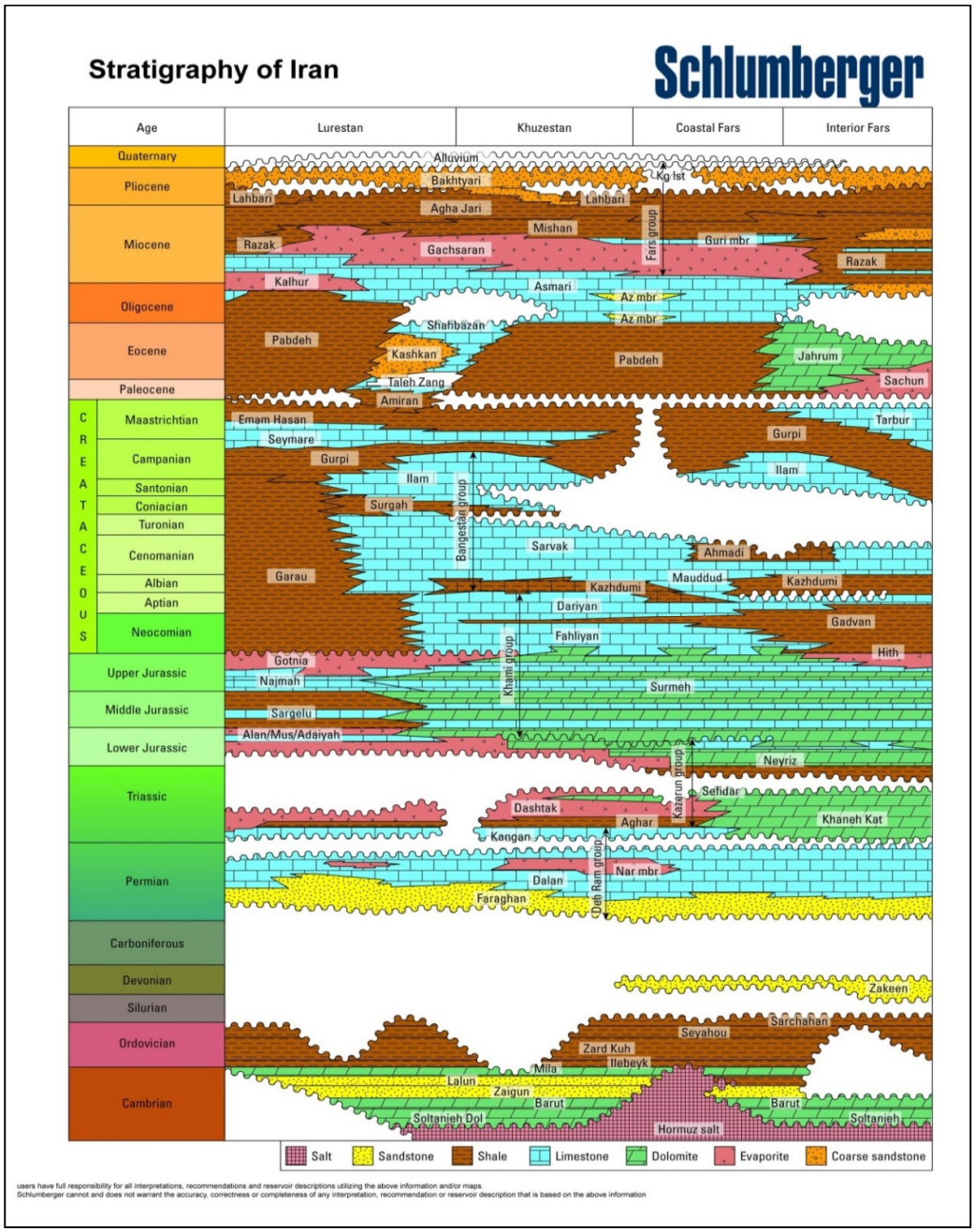

Figure 2: Gachsaran field overlying the Asmari, Pabdeh, Gurpi and other reservoirs and stratigraphic nomenclature of rock units and age relationships in the Zagros basin [2].

Penerbit Akademia Baru

Journal of Advanced Research in Applied Mechanics
ISSN (online): 2289-7895 | Vol. 10, No. 1. Pages 9-29, 2015

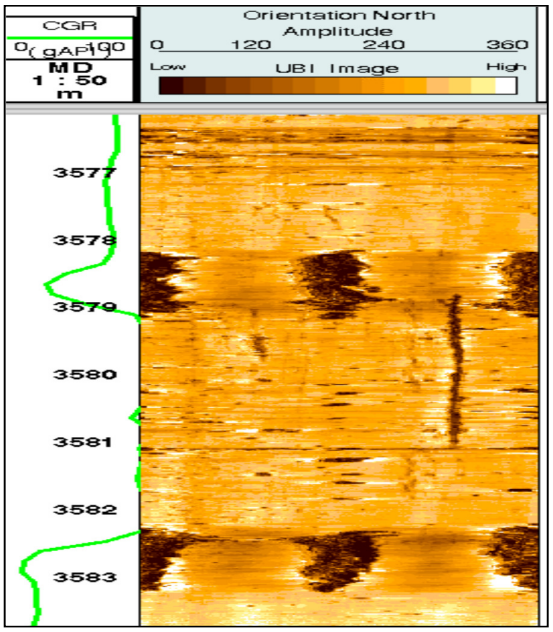

Figure 3: UBI image showing borehole breakouts and drilling induced fractures; the thin dark colour region is drilling induced fracture, and the dark wide regions are borehole breakouts.

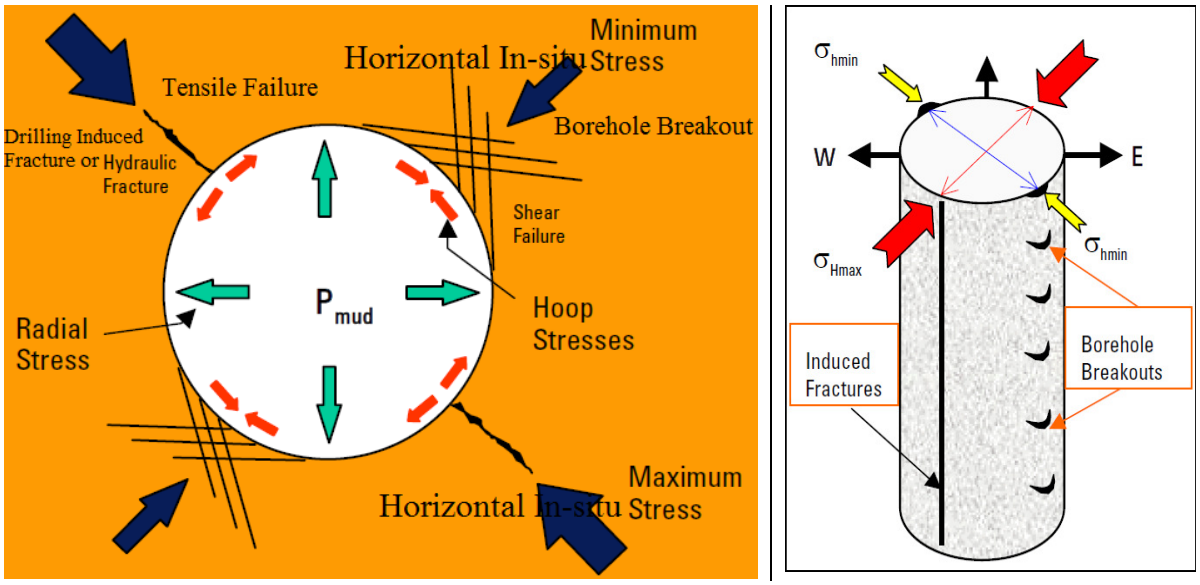

Figure 4: Schematic pictures of the radial stress, tensile failure, drilling induced fracture (hydraulic fracture), maximum horizontal stress, hoop stress, shear failure, borehole breakout and minimum horizontal stress.

Penerbit Akademia Baru

Journal of Advanced Research in Applied Mechanics
ISSN (online): 2289-7895 | Vol. 10, No. 1. Pages 9-29, 2015

4.0 RESULTS

4.1 In-situ Stress Analysis for the GS-A Well

The FMI images show borehole breakouts on the images facing northwest and southeast sides of the borehole. Thus they indicate WNW-ESE trending elliptical borehole breakouts are aligned with σ_{hmin} (Figure 5). In this well the direction of σ_{hmax} is NNE-SSW.

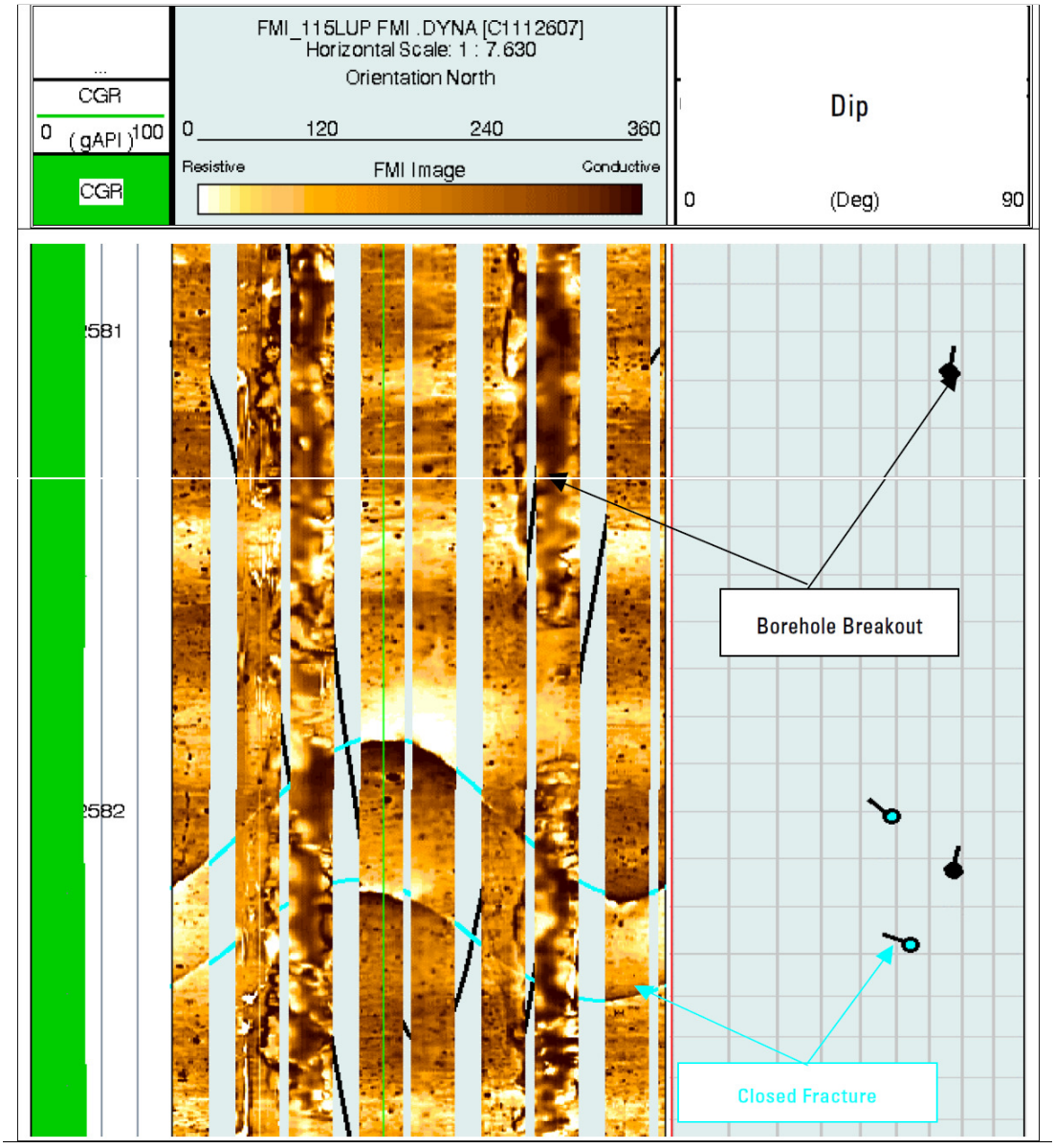

Figure 5: FMI images showing borehole breakouts in the GS-A well.

4.2 In-situ Stress Analysis for the GS-B Well

The amplitude and the radii images of UBI show elliptical borehole breakouts in many zones. In some places only the first stage of borehole breakouts in the form of conjugated shear fractures was identified. The cross-sectional slices of borehole radii across such intervals

Penerbit Akademia Baru

Journal of Advanced Research in Applied Mechanics
ISSN (online): 2289-7895 | Vol. 10, No. 1. Pages 9-29, 2015

indicate the NE-SW orientation for the longer axis of the borehole breakouts (Figure 6). It indicates the NE-SW orientation for σ_{hmin} and the NW-SE orientation for σ_{hmax}.

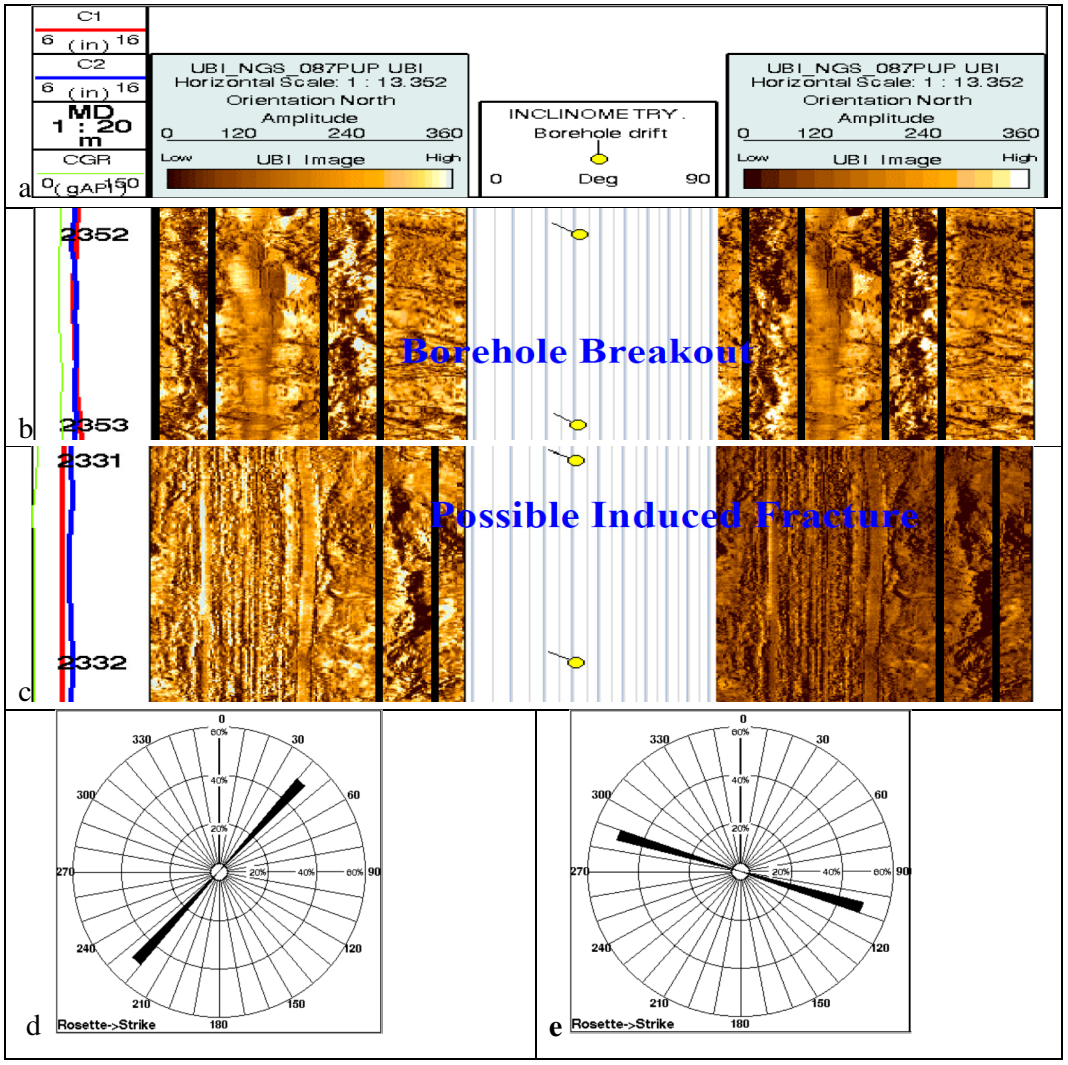

Figure 6: a) UBI log header in the GS-B well; b & c) UBI images showing borehole breakouts striking almost NE-SW, which is parallel to σ_{hmin}, and the orientation of the drilling induced fractures that is WNW-ESE to be parallel to σ_{hmax} orientation; d) strike of σ_{hmin} in Schmidt projection & e) strike of σ_{hmax} in Schmidt projection.

4.3 In-situ Stress Analysis for the GS-C Well

A cross-sectional slice of the borehole radii at 2512m and a spiral plot / down-looking pipe view across the 2512m-2512.3m depth indicate the WNW-ESE orientation for the longer axis of the borehole breakouts (Figure 7). Such breakouts represent shear failure of the formation exposed to the wellbore. The borehole breakouts indicate the WNW-ESE orientation for σ_{hmin} and the NNE-SSW orientation for σ_{hmax}.

Penerbit Akademia Baru

Journal of Advanced Research in Applied Mechanics
ISSN (online): 2289-7895 | Vol. 10, No. 1. Pages 9-29, 2015

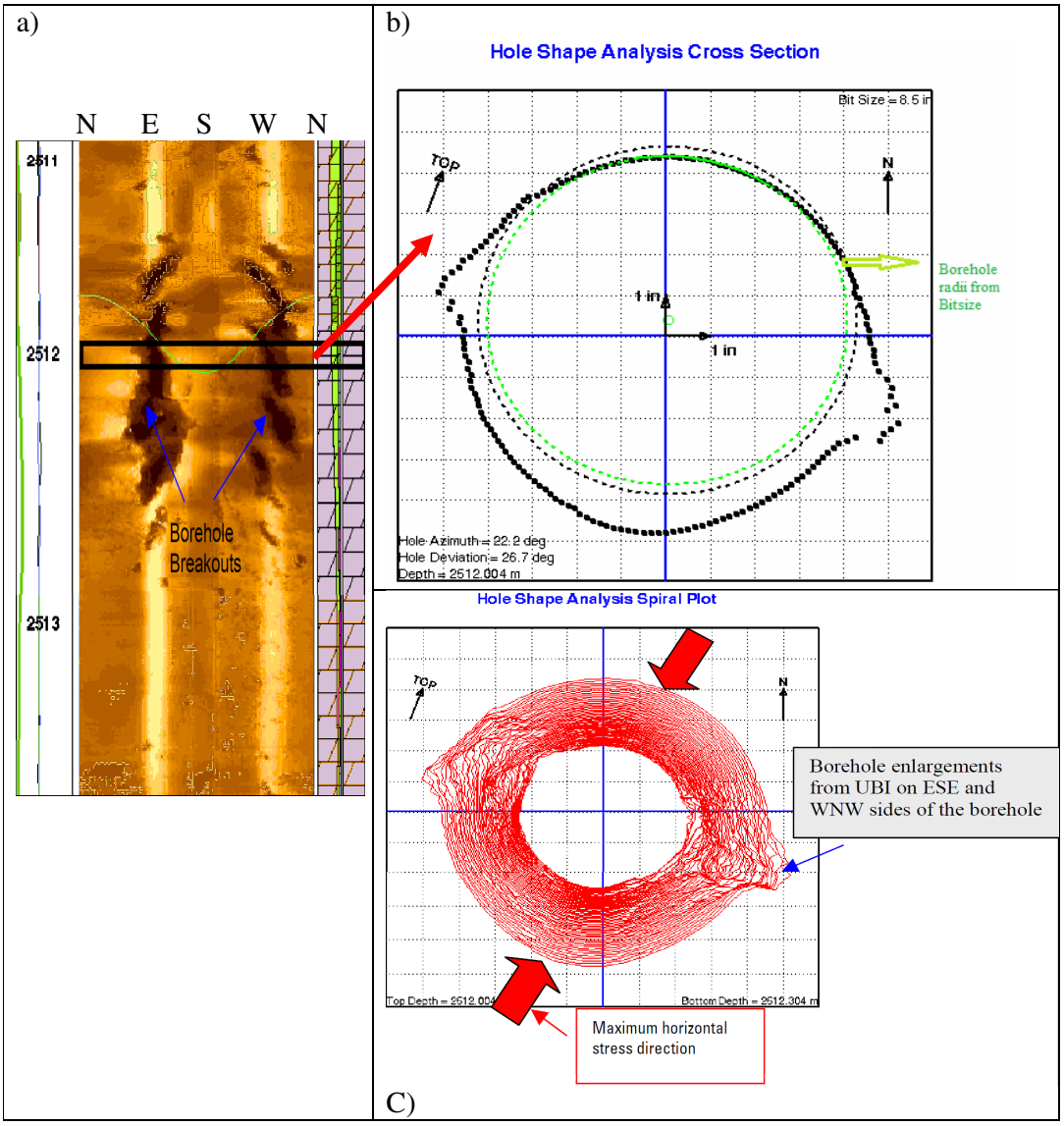

Figure 7: a) UBI image of the borehole radius showing borehole enlargements (breakouts – black vertical stripes) around WNW and ESE sides of the borehole in the GS-C well; b) and c) The down-looking pipe views of the borehole radii from the UBI.

4.4 In-situ Stress Analysis for the GS-D Well

The amplitude and radii images of UBI show elliptical borehole breakouts in most part of the borehole. A composite plot of the borehole breakout azimuth and its magnitude indicate changes in the orientation of the longer axis of the borehole breakouts. In the zones of the borehole deviation, the dominant orientation for their longer axis is the NE-SW direction (Figure 8).

Penerbit Akademia Baru

Journal of Advanced Research in Applied Mechanics
ISSN (online): 2289-7895 | Vol. 10, No. 1. Pages 9-29, 2015

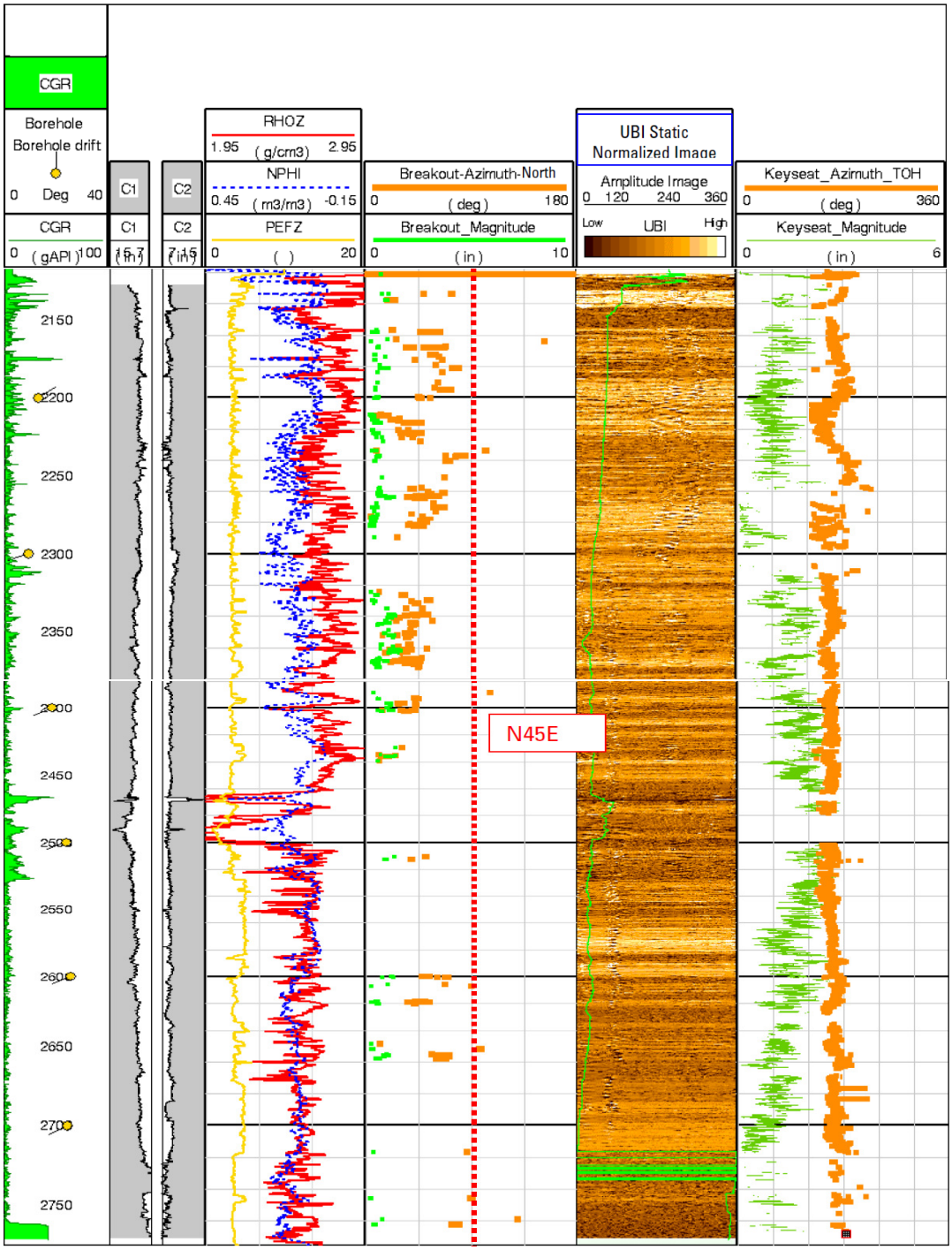

Figure 8: The composite plot of calipers and full set logs showing the borehole breakout and key seat azimuths and magnitudes in the GS-D well, which were derived from UBI images. The average breakout azimuth is N45E for the intervals with well deviation less than 20 degrees. Breakout azimuths in intervals with inclination higher than 20 degrees do not represent the exact orientation of breakouts. In such cases, breakout orientations need to be corrected.

Journal of Advanced Research in Applied Mechanics
ISSN (online): 2289-7895 | Vol. 10, No. 1. Pages 9-29, 2015

Their orientation in the zones (for example, the lower half of the well trajectory) of a well deviation greater than 20 degrees does not reflect the true orientation of borehole breakouts. A correction needs to be applied to get the true orientation of borehole breakouts in such situations. Such breakouts represent the shear failure of the formation exposed to the wellbore. Borehole breakouts indicate the NE-SW orientation for σ_{hmin} and the NW-SE orientation for σ_{hmax}.

4.5 In-situ Stress Analysis for the GS-E Well

Two drilling induced fractures were observed in the upper section of the Asmari reservoir at 2508m and 2543m. The strike direction of these fractures is N45E-S45W, which roughly indicates that the orientation of σ_{hmax} around the well is NE-SW and the orientation of σ_{hmin} is NW-SE (Figures 9 to 11).

4.6 In-situ Stress Analysis for the GS-F Well

No drill-induced fractures were observed in this well. However, a number of elliptical borehole breakouts, due to the shear failure of the borehole wall, were observed in the lower interval of the well at 2324m-2450m (Figures 12 and 13). Only a few such features were identified in the remaining interval of the Asmari formation. The large majority of these elliptical breakouts have their longer axis orientation in the NW-SE direction, which indicates that the orientation of σ_{hmin} around the well is NW-SE and the orientation of σ_{hmax} is NE-SW.

4.7 In-situ Stress Analysis for the GS-G Well

The borehole breakouts were observed in this well. They are almost in a whole interval and most of them exist in Gurpi and Pabdeh formations. There are five induced fractures with a N15E-S15W strike that shows the direction of maximum horizontal in-situ stress (Figures 14 and 15). The large majority of these elliptical breakouts have their longer axis oriented in almost the WNW-ESE direction, which indicates the orientation of σ_{hmin} around the well, therefore the orientation of σ_{hmax} will be almost in the NNE-SSW.

4.8 In-situ Stress Analysis for the GS-H Well

The borehole breakouts were observed in the whole interval of the well and most of them exist in the Gurpi and Pabdeh formations (Figures 16 and 17). The large majority of these elliptical breakouts have their longer axis orientation in almost N-E direction which indicates that the orientation of σ_{hmin} around this well is almost N-E and the orientation of σ_{hmax} is N-S (N33E-S33W for σ_{hmax} and N57W-S57E for σ_{hmin} to be more precise).

Penerbit Akademia Baru

Journal of Advanced Research in Applied Mechanics
ISSN (online): 2289-7895 | Vol. 10, No. 1. Pages 9-29, 2015

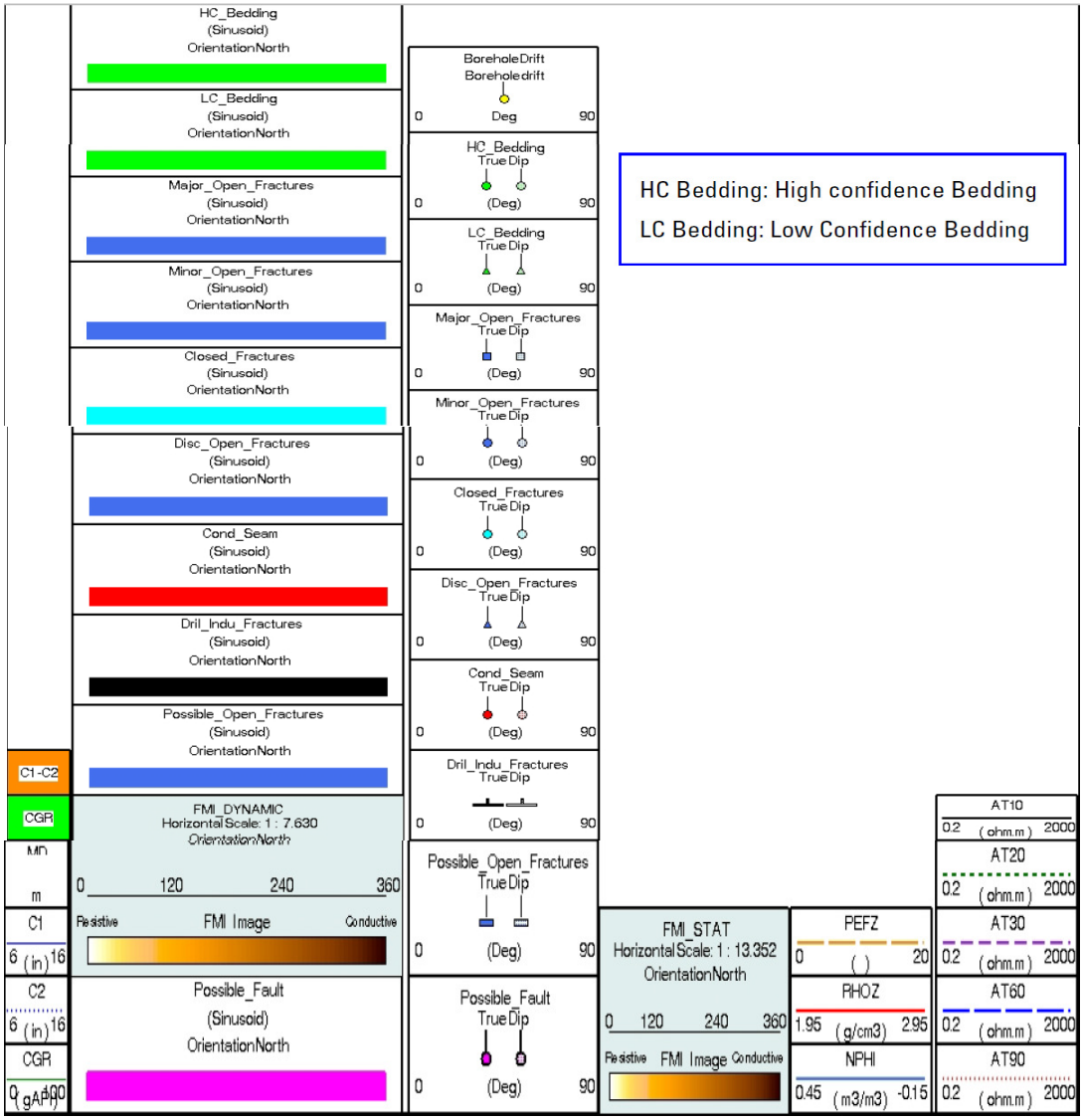

Figure 9: Header details for figures 10 and 11.

Penerbit
Akademia Baru

Journal of Advanced Research in Applied Mechanics
ISSN (online): 2289-7895 | Vol. 10, No. 1. Pages 9-29, 2015

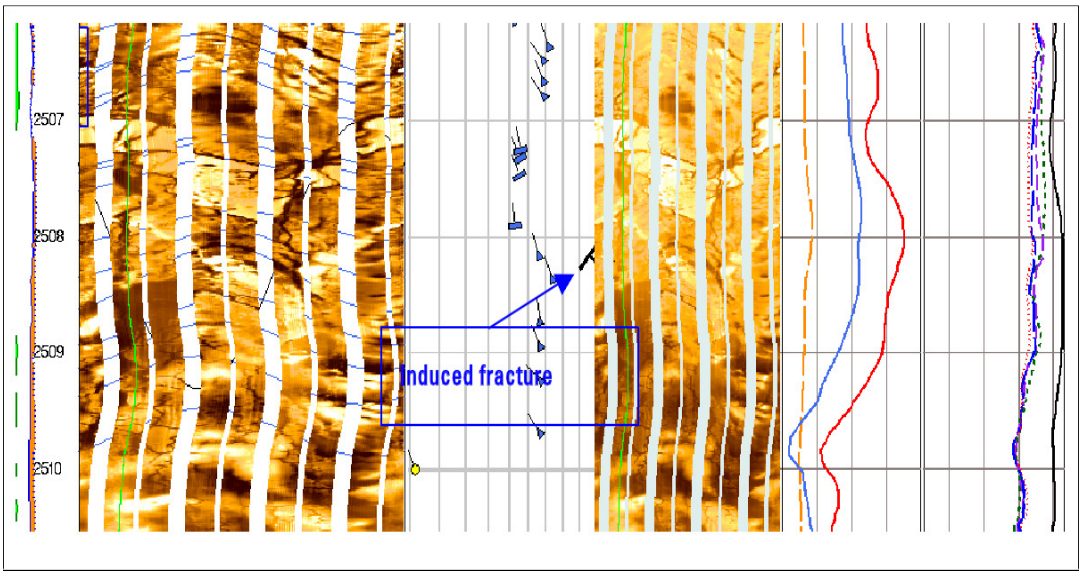

Figure 10: Images showing the NE-SW trend for the drilling induced fractures in 2508m depth in the GS-E well; header is given in Figure 9.

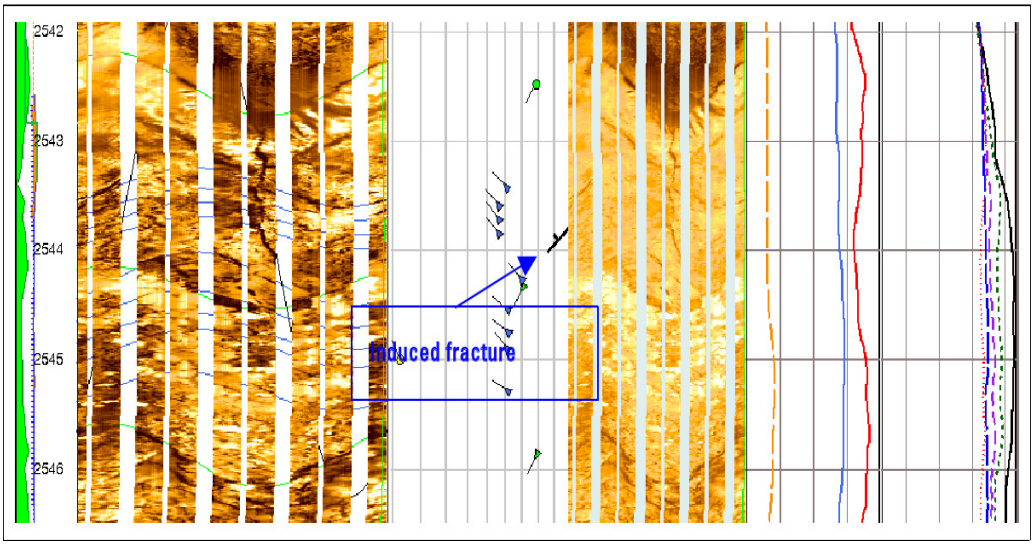

Figure 11: Images showing the NE-SW trend for the drilling induced fractures in 2543m depth in the GS-E well; header is given in Figure 9.

Penerbit Akademia Baru

Journal of Advanced Research in Applied Mechanics
ISSN (online): 2289-7895 | Vol. 10, No. 1. Pages 9-29, 2015

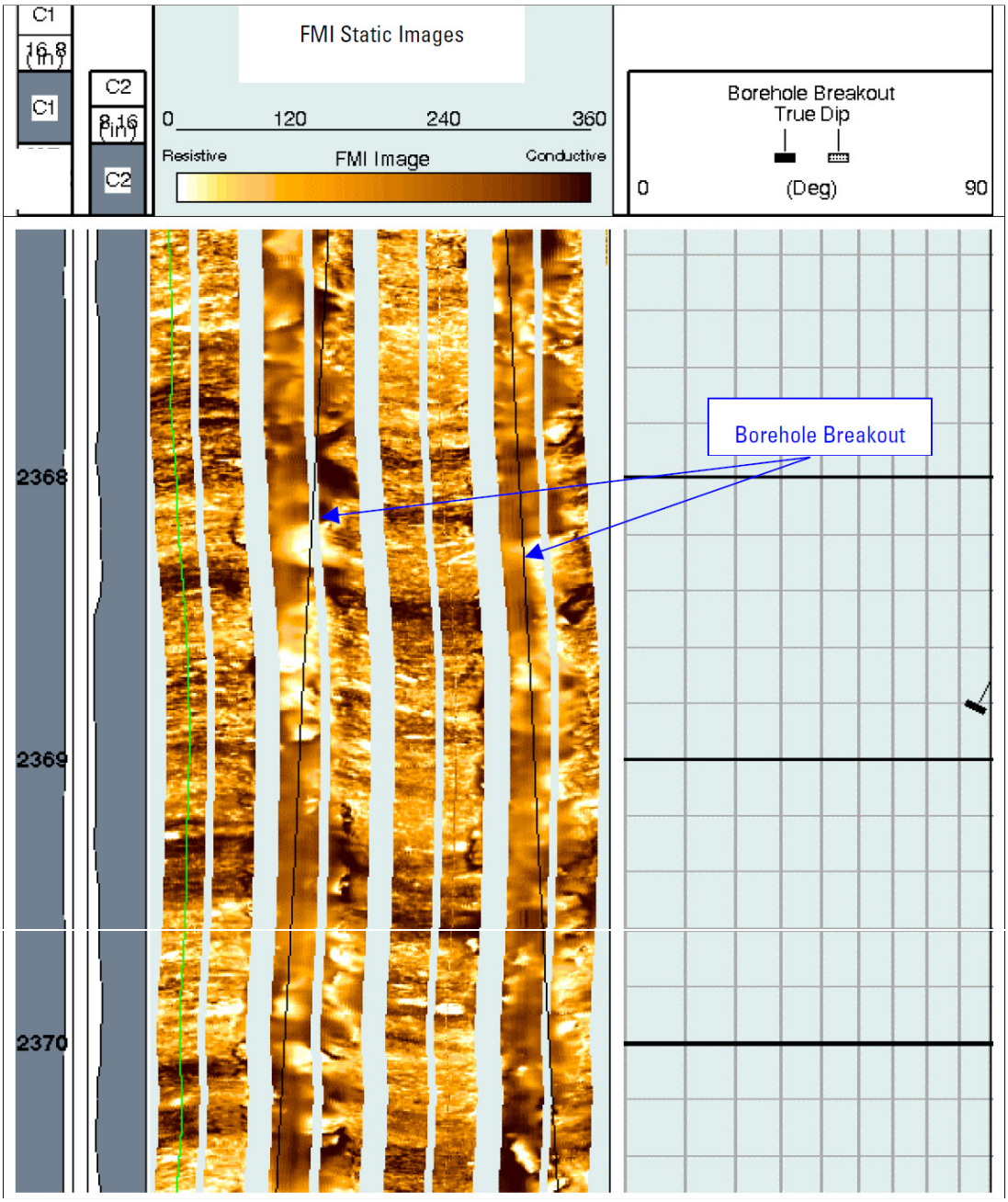

Figure 12: FMI images showing borehole breakouts on the images facing northwest (N60W to be more precise) and southeast (S60E to be more precise) sides of the borehole in the GS-F well. Thus they indicate N60W-S60E trending for σhmin.

Penerbit Akademia Baru

Journal of Advanced Research in Applied Mechanics
ISSN (online): 2289-7895 | Vol. 10, No. 1. Pages 9-29, 2015

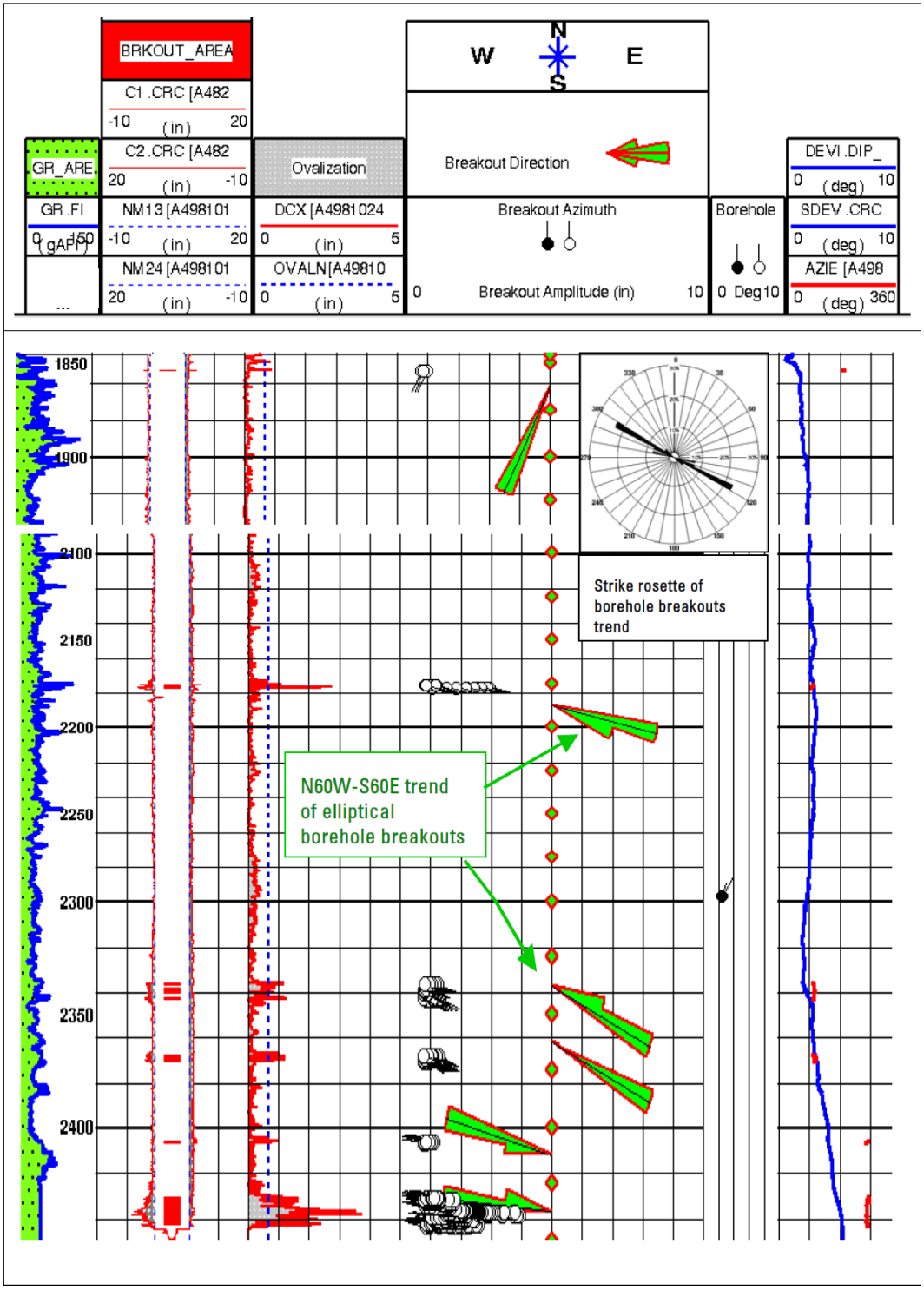

Figure 13: Logs showing dominant N60W-S60E trending for borehole breakouts in Asmari formation in the GS-F well. The breakouts were mostly observed in the lower section. These indicate the orientation of σhmin is N60W-S60E and the orientation of σhmax is N30E-S30W.

Penerbit Akademia Baru

Journal of Advanced Research in Applied Mechanics
ISSN (online): 2289-7895 | Vol. 10, No. 1. Pages 9-29, 2015

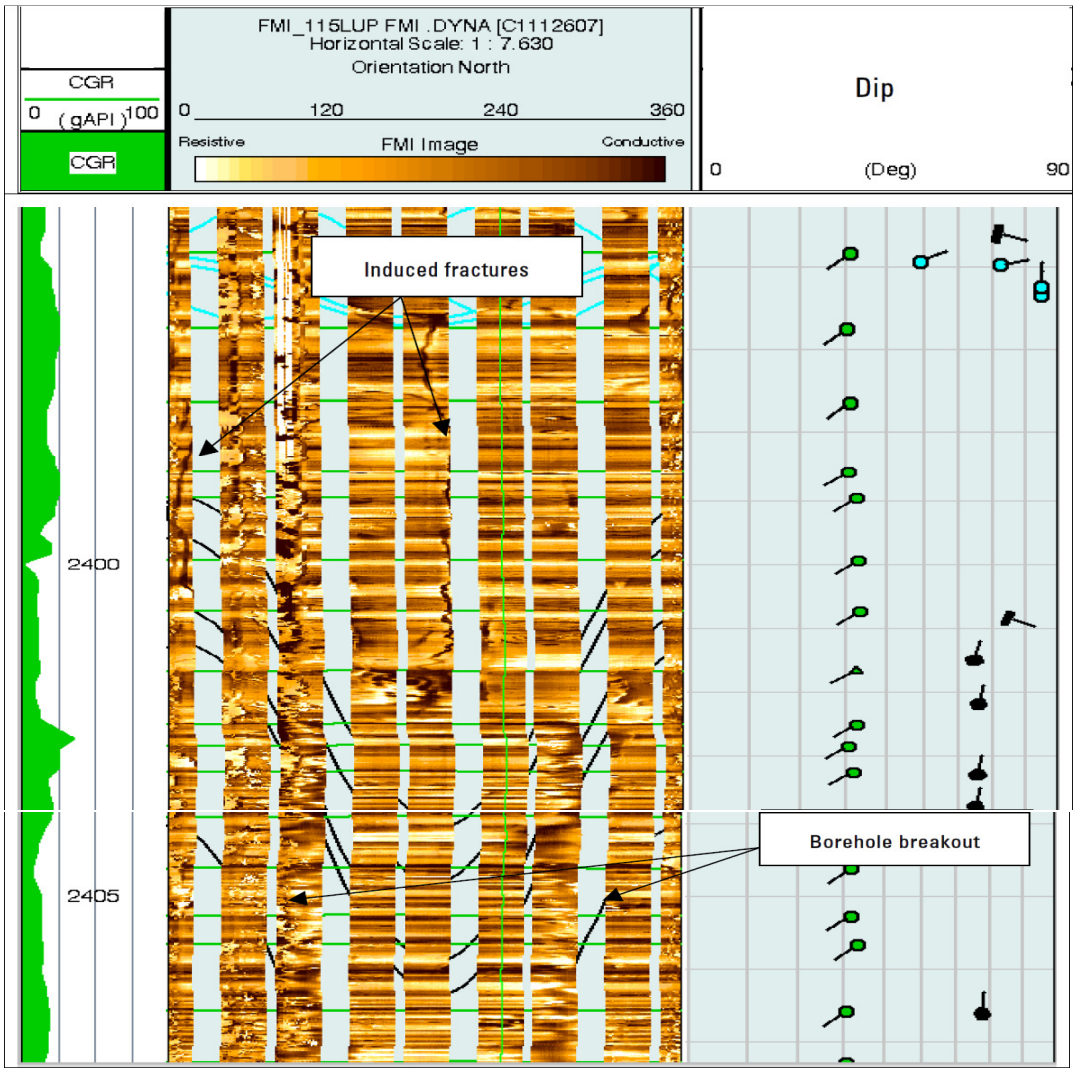

Figure 14: FMI images showing induced fractures in the upper part of the figure (2395m-2402m) and borehole breakouts in lower part (2402m-2407m) in the GS-G well. They show 90 degrees difference in the azimuth.

Penerbit Akademia Baru

Journal of Advanced Research in Applied Mechanics
ISSN (online): 2289-7895 | Vol. 10, No. 1. Pages 9-29, 2015

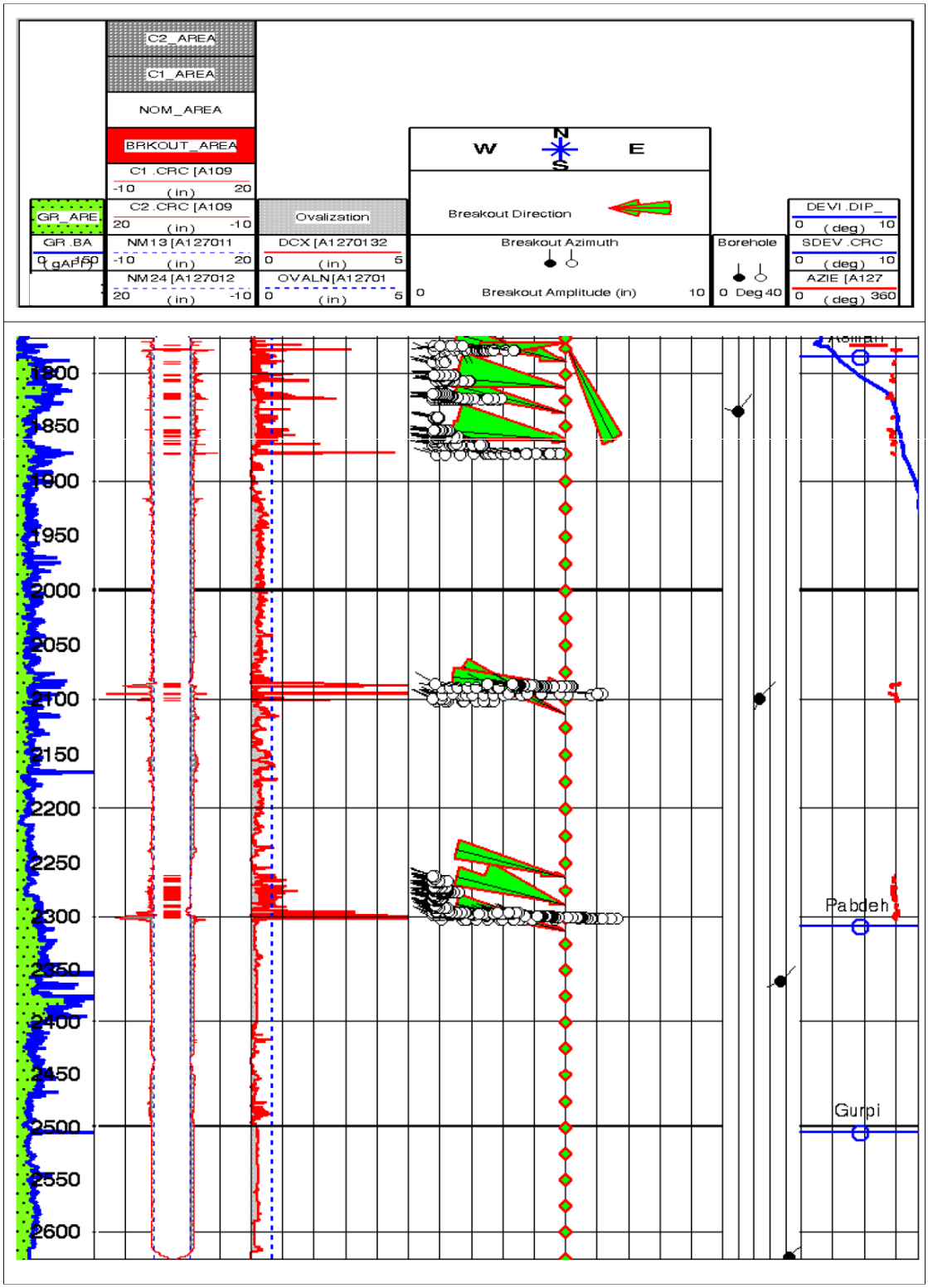

Figure 15: Logs showing the WNW-ESE trend for borehole breakouts in the Asmari formation in the GS-G well. This shows the orientation of σ_{hmin} is WNW-ESE and the orientation of σ_{hmax} is NNE-SSW.

Penerbit Akademia Baru

Journal of Advanced Research in Applied Mechanics
ISSN (online): 2289-7895 | Vol. 10, No. 1. Pages 9-29, 2015

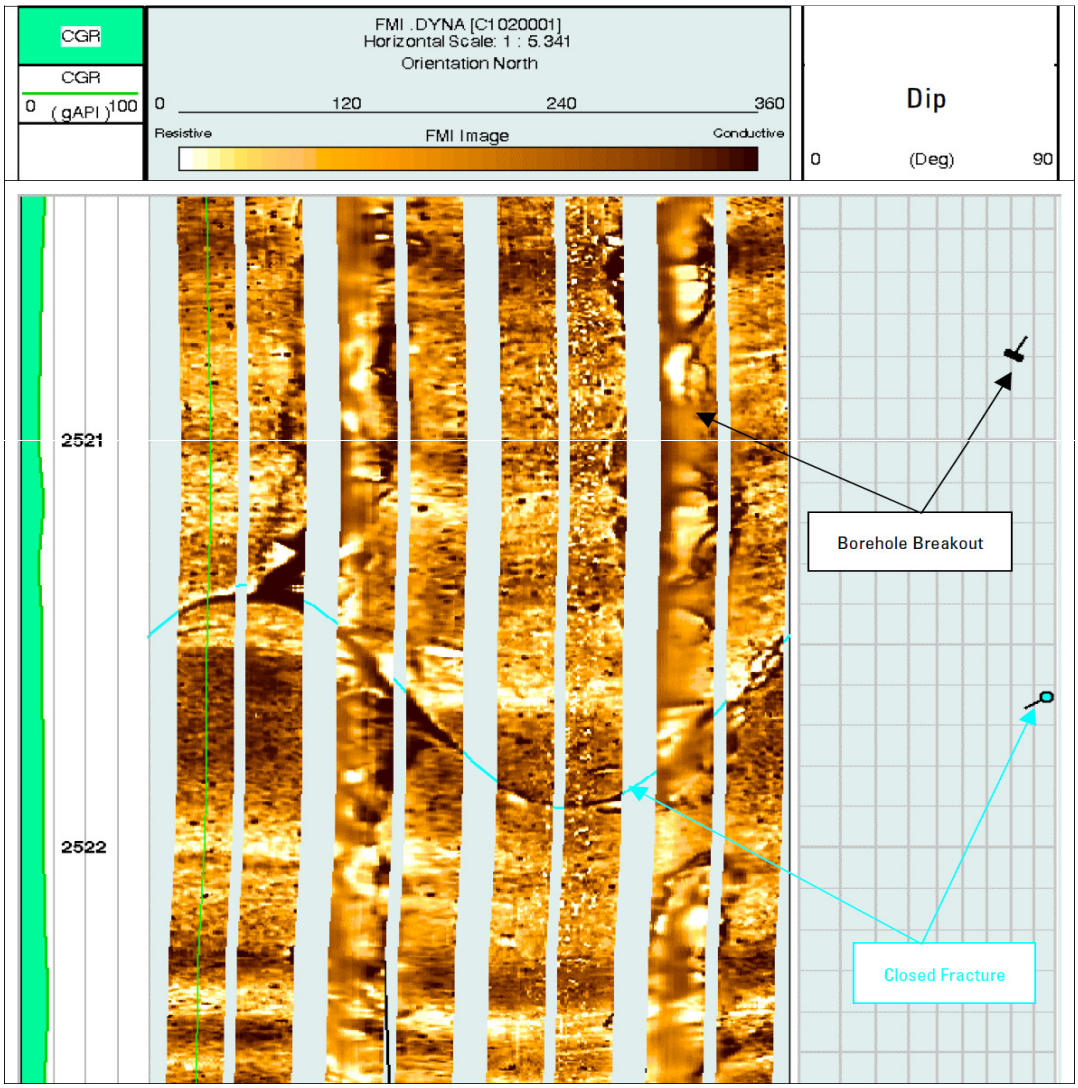

Figure 16: FMI images showing borehole breakouts facing northwest (N57W to be more precise) and southeast (S57E to be more precise) sides of the borehole in the GS-H well. Thus they indicate N57W-S57E trending elliptical borehole breakouts that are aligned with σ_{hmin}.

Penerbit Akademia Baru

Journal of Advanced Research in Applied Mechanics
ISSN (online): 2289-7895 | Vol. 10, No. 1. Pages 9-29, 2015

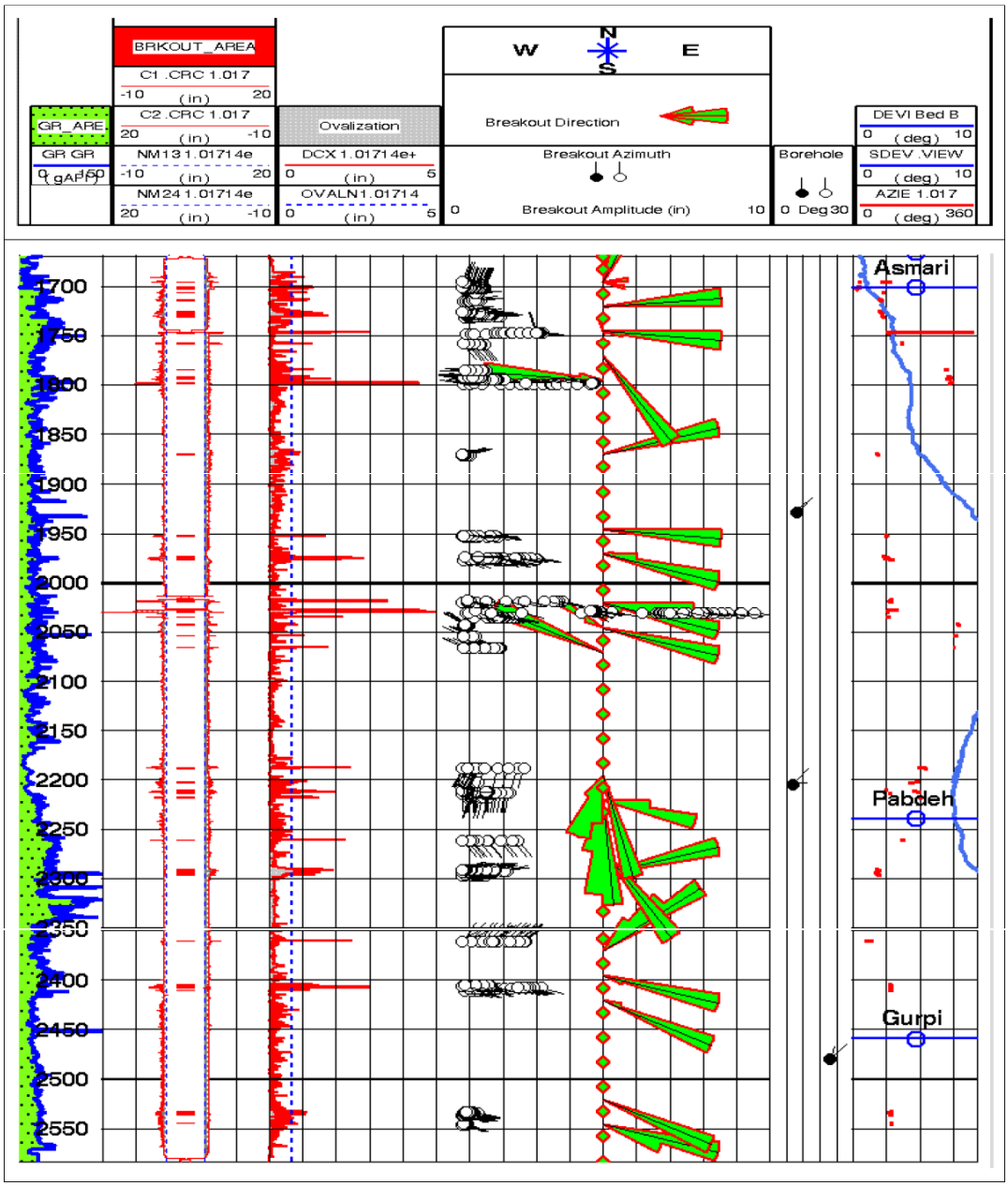

Figure 17: Logs showing E-W trend for the borehole breakouts in the Asmari formation and the NW-SE trend in the Pabdeh and Gurpi formations in the GS-H well. The breakouts were mostly observed in the Pabdeh formation. The borehole trend in Pabdeh formation is slightly different from the Asmari formation. These indicate the overall orientation of σ_{hmin} is N57W-S57E and the orientation of σ_{hmax} is N33E-S33W.

4.9 In-situ Stress Analysis for the GS-I Well

The amplitude and radii images of the UBI do not show elliptical borehole breakouts in the Asmari formation, but a few drilling induced fractures were identified (Figure 18). The orientation of the induced fractures is nearly N10E-S10W. It indicates the N10E-S10W orientation for σ_{hmax} and the N80W-S80E orientation for σ_{hmin}.

Penerbit Akademia Baru

Journal of Advanced Research in Applied Mechanics
ISSN (online): 2289-7895 | Vol. 10, No. 1. Pages 9-29, 2015

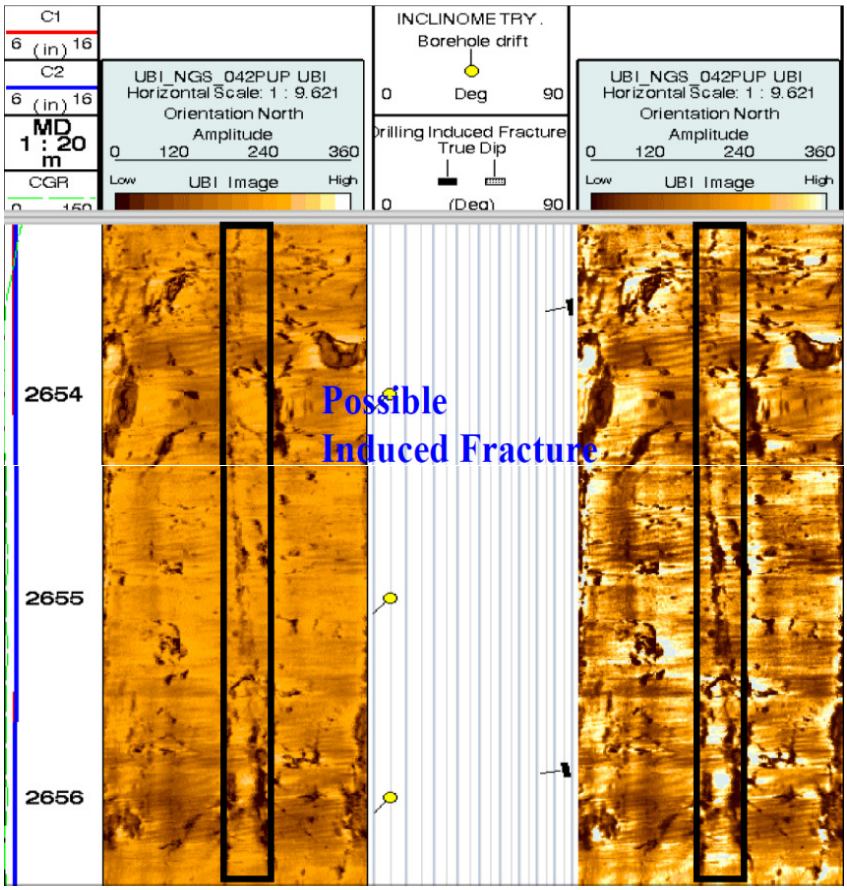

Figure 18: UBI image showing drilling induced fractures in the well GS-I.

4.10 In-situ Stress Analysis for the GS-J Well

The FMI images show induced fracture on the images facing northeast and southwest sides of the borehole. Thus they indicate NNE-SSW trending elliptical induced fractures that are aligned with σ_{hmax} (Figure 19). The direction of σ_{hmin} is NNW-SSE.

5.0 DISCUSSION

In Gachsaran field, the GS-A, GS-C, GS-E, GS-F, GS-G, GS-H and GS-I wells almost follow the NE-SW direction for maximum horizontal in-situ stress direction, and NW-SE for minimum horizontal in-situ stress direction. It shows that for this field, the direction of maximum horizontal in-situ stress is NE-SW, and the direction of minimum horizontal in-situ stress is NW-SE.

The in-situ stresses direction for the GS-B and GS-D wells are quite different from other wells, and the reason might be the effects of fault, fold and diapirism near these wells (Figure 20). For these two wells, further structural analysis and fault interpretation are needed to find out the exact reason for this difference.

Penerbit Akademia Baru
Journal of Advanced Research in Applied Mechanics
ISSN (online): 2289-7895 | Vol. 10, No. 1. Pages 9-29, 2015

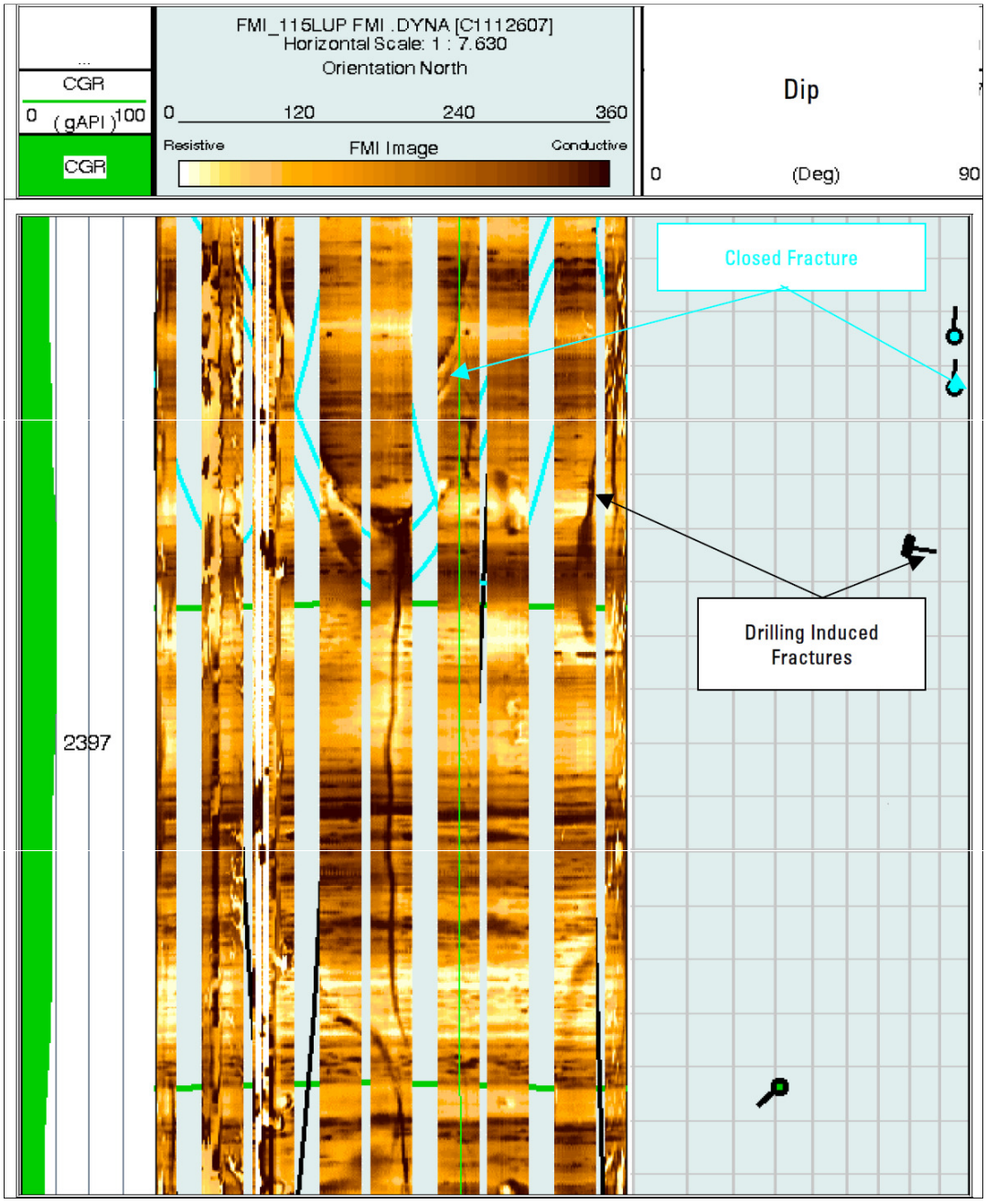

Figure 19: FMI images in the GS-J well showing induced fractures.

Penerbit Akademia Baru

Journal of Advanced Research in Applied Mechanics
ISSN (online): 2289-7895 | Vol. 10, No. 1. Pages 9-29, 2015

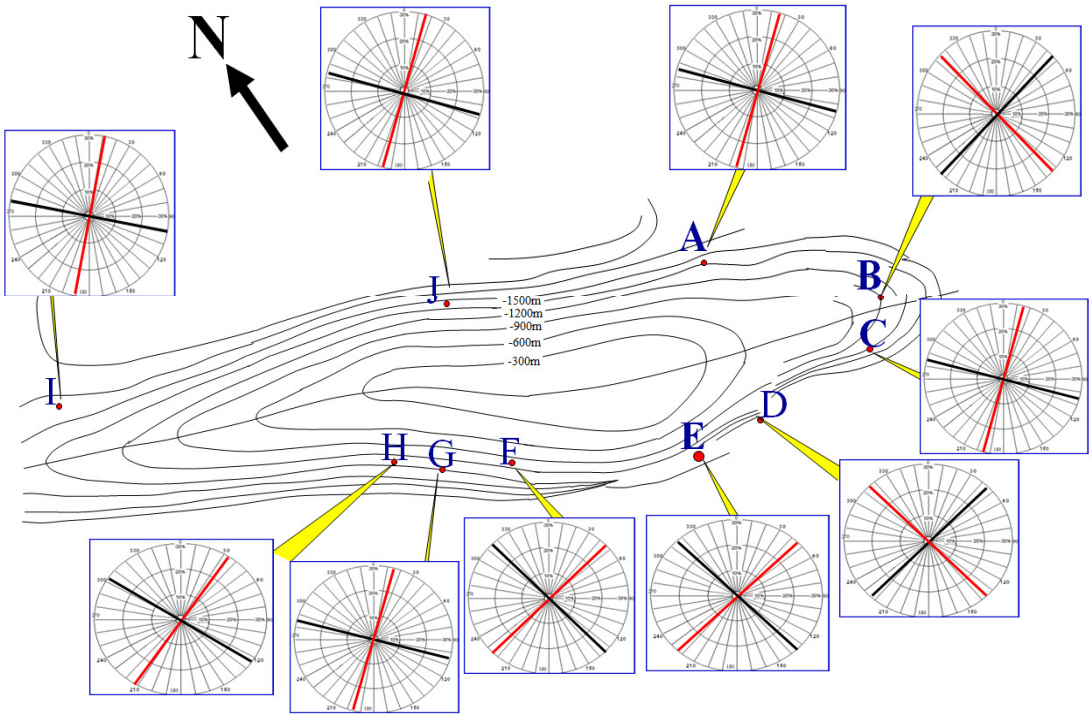

Figure 20: σ_{hmin} direction (black colour) and σ_{hmax} direction (red colour) for all the studied wells in Gachsaran field.

6.0 CONCLUSION

This work discovered the direction of drilling induced fractures and borehole breakouts of Gachsaran field, NE-SW for drilling induced fractures (maximum horizontal in-situ stress) and NW-SE for borehole breakouts (minimum horizontal in-situ stress). By having the results of this job, any hydraulic fracturing operation, EOR operations, drilling operations and the other operations in this field can be planned more accurately.

REFERENCES

[1] F. Khoshbakht, H. Memarian, M. Mohammadnia, Comparison of Asmari, Pabdeh and Gurpi formation's fractures, derived from image log, Journal of Petroleum Science and Engineering 67 (2009) 65-74.

[2] M. Alizadeh, Z. Movahed, R. Junin, W.R. Wan Sulaiman, M.Z. Jaafare, Fault interpretation using image logs, Applied Mechanics and Materials 695 (2014) 840-843.

[3] Z. Movahed, Enhanced reservoir description in carbonate and clastic reservoirs, Presented at the SPE Asia Pacific oil & Gas Conference and Exhibition. Jakarta, Indonesia, 30 October-1 November (2007).

Journal of Advanced Research in Applied Mechanics
ISSN (online): 2289-7895 | Vol. 10, No. 1. Pages 9-29, 2015

[4] M. Alizadeh, Z. Movahed, R. Junin, W.R. Wan Sulaiman, M.Z. Jaafare, Image logs application for locating faults in oil and gas reservoirs, Advanced Research in Applied Mechanics 3 (2015) 1-8.

[5] W. Lina, E. Yehb, J. Hungc, B. Haimsond, T. Hironoe, Localized rotation of principal stress around faults and fractures determined from borehole breakouts in hole B of the Taiwan Chelungpu-fault Drilling Project (TCDP), Tectonophysics 482 (2010) 82-91.

[6] X. Nie, C. Zou, L. Pan, Z. Huang, D. Liu, Fracture analysis and determination of in-situ stress direction from resistivity and acoustic image logs and core data in the Wenchuan Earthquake Fault Scientific Drilling Borehole-2 (50–1370 m), Tectonophysics 593 (2013) 161–171.

[7] Z. Movahed, R. Junin, Z. Safarkhanlou, M. Akbar, Formation evaluation in Dezful embayment of Iran using oil-based-mud imaging techniques. J. Petrol. Sci. Eng. 121 (2014) 23-37.

[8] B. Aadnoy, R. Looyeh, 2011. Petroleum Rock Mechanics, Drilling operations and Well Design. GULF Publishing Company, Houston, Texas, United States.